Size-dependent magnetic properties of VO_2 nanocrystals dispersed in a silica matrix

2008 J. Phys.: Condens. Matter 20 255202

(http://iopscience.iop.org/0953-8984/20/25/255202)

J. Phys.: Condens. Matter **20** (2008) 255202 (9pp) doi:10.1088/0953-8984/20/25/255202

Size-dependent magnetic properties of VO_2 nanocrystals dispersed in a silica matrix

Sudip Mukherjee and Arun Kumar Pal

Department of Solid State Physics, Indian Association for the Cultivation of Science, Jadavpur, Kolkata-700 032, India

E-mail: sudip.m07@gmail.com

Received 16 January 2008, in final form 14 April 2008
Published 19 May 2008
Online at stacks.iop.org/JPhysCM/20/255202

Abstract

Magnetic nanocrystalline VO_2 particles have been successfully synthesized in a silica glass matrix by the sol–gel method at calcination temperatures of 700 °C and above. The presence of small quantities of diamagnetic V_2O_5 nanocrystals in glass samples calcined at $\geqslant$800 °C has been confirmed. The thermal behavior of magnetization (zero-field-cooled and field-cooled) and magnetic hysteresis of VO_2 nanocrystals in the 10–300 K temperature interval have demonstrated that the VO_2 nanocrystals present in these glasses display superparamagnetic–ferromagnetic transition at low temperatures. X-band electron paramagnetic resonance (EPR) spectra of VO_2 nanoparticles have depicted broad symmetric lines [$\Delta H_{pp}\sim$104 mT at room temperature (RT) and 250 mT at liquid nitrogen temperature (LNT)]. The increase in EPR line intensity on going from RT to LNT suggests that VO_2 nanocrystals have undergone ferromagnetic-like ordering in the temperature interval RT–77 K. The presence of small numbers of isolated VO^{2+} ions in the SiO_2 matrix has also been confirmed from EPR studies. From EPR and optical spectral studies it has been shown that the VO^{2+} ion has square pyramidal conformation with tetragonal compression having C_{4v} symmetry. It is established that the in-plane σ bonding and out-of-plane π bonding are predominantly ionic in nature.

1. Introduction

Sol–gel processing of inorganic oxide glasses offers many advantages over the traditional melt processing techniques, such as greater homogeneity and purity, lower processing temperature and better control over glass properties. Oxide glasses and ceramic oxides prepared by the sol–gel method have optical, mechanical and electrical properties which may have practical applications [1]. Some of these applications result from the incorporation of transition metal ions in sol–gel derived materials. Electron paramagnetic resonance (EPR) of doped transition metal (TM) ions in various glasses has paved the way to understanding certain structural features of sol–gel glasses. Some dopant TM ions can be employed not only as indicators of the structure but also to explore dynamic phenomena involved in the sol–gel process. EPR of dopant TM ions has provided useful information on the structural changes in compounds during sol–gel glass/ceramic transformation and on the products formed in the sol–gel materials. Vanadium is one of the transition group elements that has been studied with EPR spectroscopy in divalent, trivalent and tetravalent states. In its tetravalent state, V^{4+} exists as a VO^{2+} ion with a single unpaired d electron [2–4]. The VO^{2+} ion is one of the most stable cations among a few molecular paramagnetic transition metal ions and is used extensively as an impurity probe for EPR studies, which are sensitive to the crystal environments. The behavior of unpaired electrons in VO^{2+} complexes is dominated by the strong V=O bonding and as a result most of the complexes possess square pyramidal symmetry (C_{4v}) and both g and A values are found to be axially symmetric. VO^{2+} complexes have been a subject of interest for a number of workers in recent years [5–9]. EPR spectra of V^{4+} ions have been studied by Bogomolova and Jachkin [7] in binary RO–B_2O_3 glasses (where R = Ba, Sr, Pb and Zn) and in ternary PbO–ZnO–B_2O_3 glasses. The superposition of two distinct EPR spectra of V^{4+} ions in binary ZnO–B_2O_3 glasses has been observed and attributed to the two-phase structure of these glasses. Bogomolova and her group [8] also studied

EPR spectra of V^{4+} ions in phosphate glasses. Recently, the same group [9] performed computer simulation EPR studies of sol–gel derived silica glass doped with 1 wt% vanadium calcined up to 1073 K at room temperature (RT) and liquid nitrogen temperature (LNT). It was shown that the source of the EPR spectra of the doped solution of aqua-complexes of the vanadyl ion (VO^{2+}) resides in the gel pores obtained after heat treatment at temperatures $\leqslant$973 K. The number of vanadyl ions in a sample decreases with increasing calcination temperature and the remainder are immobilized on the pore surface in local environments in which the spectra of the vanadium species become undetectable.

Recently, Lopez *et al* [10] studied the size effect on the optical properties of VO_2 nanoparticles (NPs). They observed that the optical contrast between the semiconducting and metallic phases was dramatically enhanced in the visible region, presenting size-dependent optical resonances and size-dependent transition temperatures.

In the backdrop of the above EPR and optical findings on vanadyl ions and VO_2 NPs, it has been thought worthwhile to grow nanosized vanadium oxide particles in an inorganic matrix like silica (SiO_2) by adopting a sol–gel method. This may provide a convenient way to tailor vanadium oxide NPs of nearly uniform sizes and to facilitate homogeneous dispersion of these metal oxide NPs in the silica matrix. From investigations of the properties of pure silica glass prepared by the sol–gel process it has been established that silica gel becomes a porous glass when calcined at ∼400 °C and that the collapse of the pores starts at ∼700 °C and becomes nearly complete at ∼800 °C [11]. So, when silica gels doped with VO^{2+} ions are subjected to systematic heating, the collapse of the silica pores is also possibly initiated near 700 °C, which triggers isolated metal oxide ions loosely attached to the pores to be detached to form clusters, the dimensions of which may fall in the nanometer range (i.e. NPs). In the present instance, the doping level is chosen to be 2.0 mol% and VO^{2+}-doped SiO_2 glass is subjected to calcination at various temperatures up to 900 °C. The sizes of nanocrystals thus obtained are ascertained from x-ray diffraction (XRD) and transmission electron microscopy (TEM) experiments. The nanocrystals are also characterized by infrared (IR) spectroscopy. Since nanocrystalline magnetic particles obviously have a high surface-to-volume ratio their magnetic properties are likely to be significantly different from those of their bulk crystalline counterparts. In fact, below a critical nanocrystal size, superparamagnetism might occur due to the fact that the thermal energy becomes comparable to the magnetic anisotropy energy. Magnetic studies such as dc magnetizations—zero-field-cooled (ZFC) and field-cooled (FC)—and magnetic hysteresis in the magnetic field range (±5 T) are performed at various low temperatures down to 10 K to arrive at a satisfactory picture of the nature of magnetism of these NPs. EPR spectroscopy is recognized as a powerful method for exploring spin dynamics in magnetic materials including ferro-and antiferromagnets [12, 13] and spin glasses [14, 15]. The transition to the magnetically ordered state can be easily detected by the EPR method. EPR data give information about the local magnetic properties and, in principle, also about the nature of spin–spin interactions [16]. EPR of vanadyl ions in glasses is very interesting because the valence state of vanadyl changes with variation of the glass composition and melting atmosphere [17]. So, X-band EPR investigations at RT and LNT are carried out for isolated VO^{2+} ions and VO_2 NPs obtained at various calcination temperatures. The spin-Hamiltonian and molecular orbital parameters of isolated VO^{2+} ions in this host lattice are also deduced from EPR and room temperature optical absorption data to throw light on the covalent aspects of vanadyl ions in the surroundings of a silica matrix.

2. Experimental details

Vanadium-oxide-doped silica gel is prepared from tetraethylorthosilicate (TEOS) and dopant vanadyl sulfate having a 2.0 mol% dopant concentration (henceforth referred to as V2), essentially following the method of Sakka and Kamiya [18]. The molar ratio of water and TEOS is kept at 20 while that of TEOS and catalyst HCl is 100. Dry ethanol is used as a solvent. The solution, poured in a Pyrex beaker and covered with polythene sheet, is kept in the atmosphere for 7–8 days to form a stiff monolithic gel. The monolithic gel is then allowed to dry further at room temperature for 4–5 weeks. Dried gels are then transferred to a programmable electric furnace. Heat treatments of these samples are then performed in air at several pre-selected temperatures up to 900 °C, in accordance with the following schedule [19].

$$\mathrm{RT} \xrightarrow{3.5\ \mathrm{h}} 250\,^{\circ}\mathrm{C}\ (4\ \mathrm{h}) \xrightarrow{2.5\ \mathrm{h}} 310\,^{\circ}\mathrm{C}\ (4\ \mathrm{h}) \xrightarrow{2.5\ \mathrm{h}} 440\,^{\circ}\mathrm{C}\ (16\ \mathrm{h}) \xrightarrow{2.5\ \mathrm{h}} 500\,^{\circ}\mathrm{C}\ (4\ \mathrm{h}) \xrightarrow{2.5\ \mathrm{h}} 600\,^{\circ}\mathrm{C}\ (4\ \mathrm{h}) \xrightarrow{2.5\ \mathrm{h}} 700\,^{\circ}\mathrm{C}\ (4\ \mathrm{h}) \xrightarrow{2.5\ \mathrm{h}} 800\,^{\circ}\mathrm{C}\ (4\ \mathrm{h}) \xrightarrow{2.5\ \mathrm{h}} 900\,^{\circ}\mathrm{C}\ (4\ \mathrm{h}).$$

The gel glasses are removed from the furnace at pre-selected temperatures and are stored inside an oven maintained at 130 °C.

EPR spectra of V2 samples calcined at 700, 800 and 900 °C are recorded in a Varian X-band EPR spectrometer (model E-109) with 100 kHz magnetic field modulation at RT and LNT. Powder XRD spectra of V2 glass specimens are recorded using a Seifert diffractometer (model XRD3000) with a Cu Kα radiation source. An ultrahigh resolution JEOL JEM-2010 analytical TEM is employed to record TEM of V2 samples calcined at 700 and 900 °C. Samples for TEM investigation are prepared by putting a drop of ethanolic dispersion of a fine powder of V2 samples onto an amorphous carbon substrate supported on a copper grid. The IR spectra of a KBr emulsion of the samples having a thickness in the range 0.1–0.3 mm are also recorded using an IR Nicolet spectrometer (model MAGNA-IR750 series II) in the range 4000–400 cm^{-1}. Optical absorption spectra of V2 samples were recorded using a Shimadzu UV–vis spectrometer (model 2101PC) in the 200–900 nm region. The magnetization and magnetic hysteresis measurements are performed on a commercial MPMS XL (Evercool model) with temperatures varying from 10 to 300 K with ±1.0 K thermal stability and equipped with a superconducting magnet producing fields up to ±5 T.

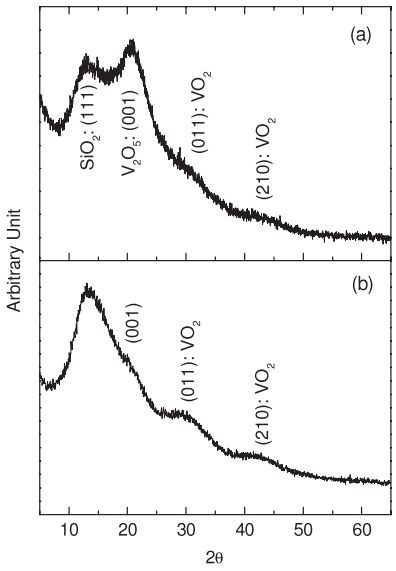

Figure 1. X-ray diffraction pattern of 2 mol% VO^{2+} doped gel glass samples calcined at (a) 900 °C and (b) 800 °C.

To carry out these measurements, the sample is packed in powder form into a pocket made from polytetrafluoroethylene (PTFE) tape and fixed to a length of copper wire. Masses of the samples are chosen in the range of 8–12 mg to obtain a good signal-to-noise ratio. V2 samples calcined at 700, 800 and 900 °C are first cooled in zero magnetic field down to 10 K and then magnetizations are recorded by increasing the temperature in an applied magnetic field of 200 Oe (ZFC measurements). FC curves are recorded by cooling the samples again in the presence of the same field. To obtain the field dependence of the magnetization, i.e. a hysteresis loop, V2 samples are cooled to a specific temperature and then the sample's magnetic moment, as a function of the magnetic field with a field stabilization time of 90 s, is recorded in the magnetic field range of ±5 T.

3. Results and discussions

3.1. XRD spectra and TEM

XRD spectra of 2 mol% VO^{2+} doped SiO_2 glass samples calcined at 800 °C and 900 °C (figure 1) are recorded at a scanning rate of 0.03° s^{-1} in the 2θ range from 5° to 65°. In each case the spectra exhibit a $2\theta = 20.27°$ (001) line, which is the signature of the crystalline phase of V_2O_5 (JCPDF no. 411426) belonging to the orthorhombic class having space group $Pmmn(59)$ and unit cell parameters $a = 11.51$ Å, $b = 3.565$ Å and $c = 4.372$ Å and a line due to the VO_2 crystalline phase at $2\theta = 27.79°$ (011) (JCPDF no. 431051) belonging to the monoclinic class (space group $P2_1/c$ (14)) and unit cell parameters $a = 5.751$ Å, $b = 4.537$ Å and $c = 5.382$ Å, $\beta = 122.64$. The only difference is that the V_2O_5 line is more prominent in the sample calcined at a higher temperature, i.e. 900 °C, which signifies that VO^{2+} clusters transform irreversibly to V_2O_5 at a greater rate at higher calcination temperatures and so V_2O_5 crystals will be present in greater numbers. V_2O_5 crystals, being diamagnetic and so insensitive to EPR, will lead to the weakening of broad signal due to the VO^{2+} crystals. This is confirmed by the EPR measurements (discussed in the EPR section).

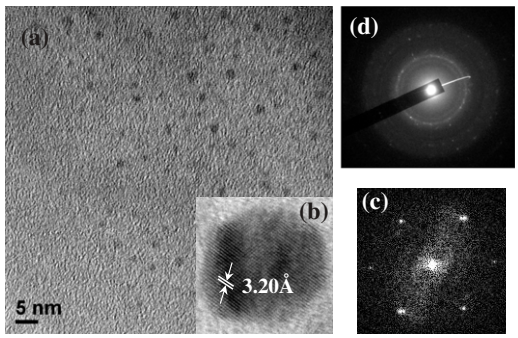

Figure 2. (a) High-magnification TEM images of VO_2 NPs calcined at 700 °C, (b) the HRTEM image, (c) the corresponding fast-Fourier transform and (d) electron diffraction patterns of TEM images.

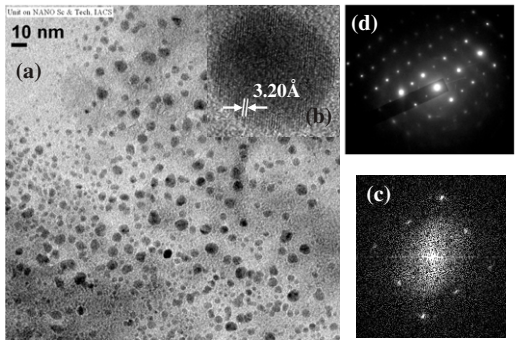

Figure 3. (a) High-magnification TEM images of VO_2 NPs calcined at 900 °C, (b) the HRTEM image, (c) the corresponding fast-Fourier transform and (d) electron diffraction patterns of TEM images.

XRD lines due to VO_2 crystals have significant line broadening, indicating that the crystal sizes are most likely to be in the nanometer range. Applying the well-known Scherrer equation, the sizes of VO_2 crystals are estimated from the integral breadths of the lines. It is confirmed that the sizes of VO_2 crystals embedded in the silica glass matrix indeed lie in the nanometer range (5–10 nm) and are larger at higher calcination temperatures. It is observed that at higher calcination temperatures the VO_2 line becomes more intense, providing evidence of increasing crystallinity at higher calcination temperatures.

TEM images of powder specimens of V2 samples calcined at 700 °C and 900 °C respectively (figures 2(a) and 3(a)) show nearly spherical NPs due to VO_2 in the range 3–10 nm. The sizes of the VO_2 NPs measured from TEM images are in fair agreement with those obtained from XRD data (table 1). The detailed structure of VO_2 is further examined by high resolution TEM (HRTEM). Representative HRTEM images of respective VO_2 NPs together with their corresponding fast-Fourier transforms (FFT) (figures 2(b) and (c) and 3(b) and (c)) show clear lattice fringes without defects or dislocations, thus providing additional confirmation that these NPs are of high crystallinity. The interplanar spacing (3.20 Å), combined with

Table 1. Powder XRD and TEM data of calcined vanadyl-doped silica glass.

Calcination temperature (°C)	Nanocrystals	XRD lines 2θ (deg.)	(hkl)	Crystal size (nm) (from XRD)	Particle size (nm) (from TEM)
700	VO_2	—	—	—	≈3
800	VO_2	27.79	(0 1 1)	≈5	—
		42.26	(2 1 0)		
	V_2O_5	20.27	(0 0 1)		—
900	VO_2	27.79	(0 1 1)	≈10	≈7
		42.26	(2 1 0)		
	V_2O_5	20.27	(0 0 1)		—

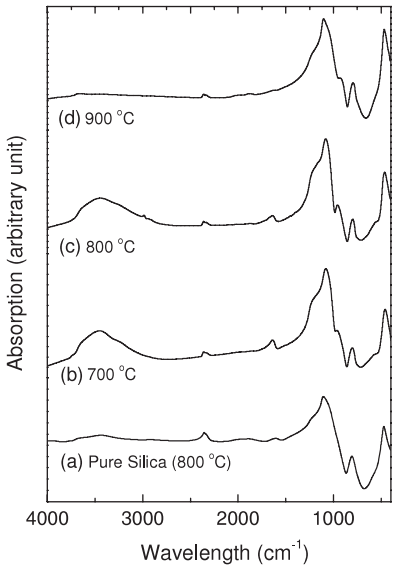

Figure 4. IR absorption spectra of vanadyl-doped silica glass at different calcination temperatures.

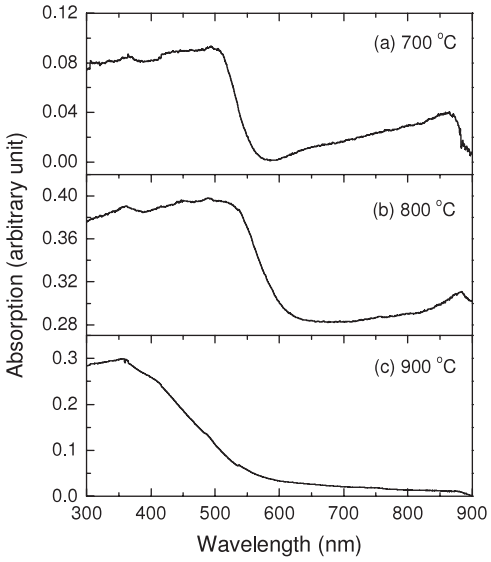

Figure 5. Optical absorption spectra of vanadyl-doped silica glass at different calcination temperatures.

the result of FFT analysis is found to be in agreement with the d spacing of the (011) plane of monoclinic VO_2. The electron diffraction patterns for the 700 °C sample shows spotted ring patterns that suggest the development of regions of localized crystallinity (figure 2(d)). For 900 °C, the diffraction patterns are very ordered symmetrical spot patterns typical of single crystal VO_2 (figure 3(d)).

3.2. Absorption spectra

3.2.1. (I) IR absorption spectra (figure 4). The salient IR spectral features of V2 samples calcined at various temperatures are as follows:

(i) The bands at ∼1220 and ∼1100 cm^{-1} are associated with the LO and TO modes of the Si–O–Si asymmetric bond stretching vibration, respectively [20], while the band at 800 cm^{-1} has been assigned to Si–O–Si symmetric bond stretching vibration and also to vibrational modes of the ring structure of SiO_4 tetrahedra. The band at ∼460 cm^{-1} is associated with a network of Si–O–Si bond bending vibrations [21]. It is significant to note that the intensities of all these IR bands increase with increasing calcination temperature.

(ii) IR lines of vanadyl-doped silica glass obtained at ∼950 cm^{-1} (samples B, C, D) are absent in the IR spectra of pure silica glass (sample A) and have been identified to arise from VO_2 crystals present in these glasses [22]. This is consistent with powder XRD findings.

3.2.2. (II) Optical absorption spectra. The optical absorption spectra at room temperature of VO^{2+} doped glass calcined at 700, 800 and 900 °C are depicted in figure 5. Three absorption bands in the UV–vis region centered at 865 nm (11 561 cm^{-1}), 650 nm (15 385 cm^{-1}) and 506 nm (19 763 cm^{-1}) are identified for the sample calcined at 700 °C. The d-energy level ordering of vanadyl complex was given by Ballhausen and Gray [23] in terms of molecular orbitals. In a C_{4v} symmetry environment (square pyramidal arrangement), the ground state is an orbital singlet and the d electron is in the non-bonding ($^2B_{2g}$) type d_{xy} orbital. The observed bands of the 700 °C calcined sample are attributed to d–d transitions [24]. On the basis of molecular orbital theory due to Ballhausen and Gray, the observed bands are assigned to transitions, $^2B_{2g} \rightarrow {}^2E_g(d_{xy} \rightarrow d_{xz,yz})$, $^2B_{2g} \rightarrow {}^2B_{1g}(d_{xy} \rightarrow d_{x^2-y^2})$ and $^2B_{2g} \rightarrow {}^2A_{1g}(d_{xy} \rightarrow d_{z^2})$ in increasing order of energy. The proposed ligand field energy scheme is shown in figure 6. The cubic field parameter D_q and

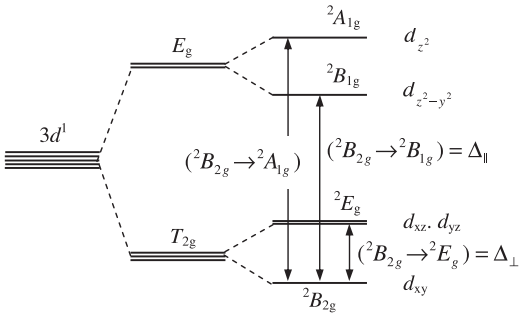

Figure 6. Schematic energy level diagram of ligand field states of the VO^{2+} ion under tetragonal distortion having C_{4v} symmetry. $\Delta_\parallel = 15\,385\ cm^{-1}$, $\Delta_\perp = 11\,561\ cm^{-1}$.

tetragonal field parameters D_s and D_t are evaluated from the following expressions:

$$^2B_{2g} \rightarrow {}^2E_g = -3D_s + 5D_t$$

$$^2B_{2g} \rightarrow {}^2B_{1g} = 10D_q$$

$$^2B_{2g} \rightarrow {}^2A_{1g} = 10D_q - 4D_s - 5D_t.$$

These parameters are evaluated as $D_q = 1539\ cm^{-1}$, $D_s = -2277\ cm^{-1}$ and $D_t = 946\ cm^{-1}$. These parameters are well comparable with the values reported for VO^{2+} ions [25–27] under tetragonal distortion. The situation is similar for the samples calcined at 800 and 900 °C. The higher-energy band ($27\,930\ cm^{-1}$) is probably the charge transfer band arising due to the promotion of one electron from the filled bonding level e_π^b to the non-bonding level b_2 [28] and shifted towards a longer wavelength in the case of samples calcined at higher temperatures. The shift of the charge transfer band implies that some of the VO^{2+} ions are transformed to a higher valence state. The presence of V_2O_5 as evident from XRD has favored the above assignment. Thus the annealing process brings out changes in the valency of vanadyl dopant ions in an oxidative way. The ligand field bands will be further discussed in connection with the EPR spectral findings presented in the next section.

3.3. EPR spectra

X-band EPR spectra of vanadium oxide doped silica glasses calcined at different temperatures were recorded at RT and LNT temperatures. Each spectrum consists of narrow lines (type-I) with a broad line (type-II) superimposed on it.

3.3.1. Type-I HF line due to isolated VO^{2+} ions doped in SiO_2 glass. In all samples with the exception of the 900 °C calcined sample (figure 7), RT EPR spectra show a well-resolved isotropic eight-line hyperfine (HF) structure with isotropic hyperfine parameter $A = 9$ mT, reasonably assigned to isolated VO^{2+} ions embedded in a glass matrix, due to the interaction of electron spin ($S = 1/2$) with the ^{51}V nucleus ($I = 7/2$) which becomes anisotropic at LNT with a 16-line feature (eight parallel and eight perpendicular

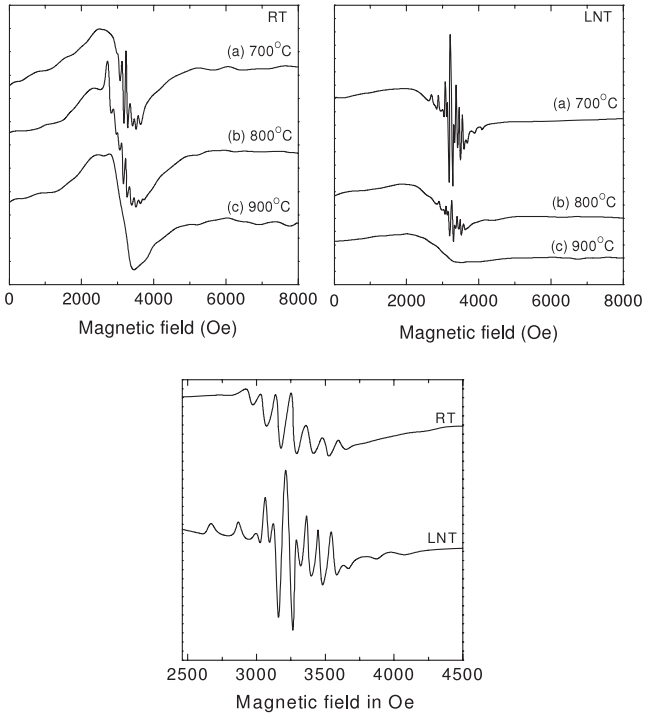

Figure 7. RT and LNT EPR spectra of 2.0 mol% VO^{2+} doped SiO_2 gel glasses at different calcination temperatures. RT and LNT hyperfine EPR spectra of 2.0 mol% VO^{2+} doped SiO_2 gel glasses calcined at 700 °C.

lines). The spectra can be best described by the well-known spin-Hamiltonian [29, 30] for vanadyl ions having an axially distorted ligand field environment with B_{2g} as the ground state:

$$\mathbf{H} = \beta[g_\parallel \mathbf{B}_z\mathbf{S}_z + g_\perp(\mathbf{B}_x\mathbf{S}_x + \mathbf{B}_y\mathbf{S}_y)] + A_\parallel \mathbf{S}_z\mathbf{I}_z + A_\perp(\mathbf{S}_x\mathbf{I}_x + \mathbf{S}_y\mathbf{I}_y)$$

where β is the Bohr magneton while $g_\parallel$, $g_\perp$ and $A_\parallel$, $A_\perp$ are the components of the gyromagnetic tensor **g** and hyperfine tensor **A**, respectively. $\mathbf{B}_x$, $\mathbf{B}_y$ and $\mathbf{B}_z$ are components of the magnetic field, S_x, S_y, S_z and $\mathbf{I}_x$, I_y, I_z are the components of the spin operators of the electron and the nucleus, respectively. The magnetic field positions of the parallel and perpendicular hyperfine peaks take into account the second order perturbation terms [31, 32], in which m is the nuclear spin magnetic quantum number which can have the values $\pm 7/2$, $\pm 5/2$, $\pm 3/2$, $\pm 1/2$. The other notations have the usual meaning.

The spin-Hamiltonian parameters ($g_\parallel$, $g_\perp$, $A_\parallel$, $A_\perp$) of the LNT spectra are derived by computer fitting: $g_\parallel = 1.93$, $g_\perp = 1.98$, $A_\parallel = 21$ mT, $A_\perp = 7.5$ mT. An octahedral site with a tetragonal compression would give values of $g_\parallel < g_\perp < g_e$ and $|A_\parallel| > |A_\perp|$ [33, 34]. The present values of the spin-Hamiltonian parameters agree with the above order. From this observation it is suggested that the paramagnetic V^{4+} ion in a glass matrix exists as the vanadyl ion, VO^{2+}, in an octahedral environment of oxygen with tetragonal distortion (C_{4v}) [35]. The V^{4+} site in the VO^{2+} ion forms coplanar bonds with each of the four oxygen ligands. The vanadyl oxygen is attached axially above the V^{4+} site along the z-axis while the sixth oxygen forming the octahedral $O\cdots VO^4\cdots O$ unit lies axially below the V^{4+} site. For all samples of VO^{2+} doped silica

Table 2. Principal g, hyperfine (A) and molecular orbital coefficients for isolated VO^{2+} ions doped in a SiO_2 glass sample calcined at 700 °C.

$g_\parallel$	$g_\perp$	$\lvert A_\parallel\rvert$ (10^{-4} cm^{-1})	$\lvert A_\perp\rvert$ (10^{-4} cm^{-1})	β_1^2	β_2^2	γ^2	$1-\beta_1^2$	$1-\gamma^2$	κ	P (10^{-4} cm^{-1})
1.93	1.98	189.2	69.3	0.88	0.92	0.81	0.12	0.19	0.74	139.5

glasses calcined at various temperatures EPR spectra are found to be composed of one broad resonance line with $\Delta H_{pp} \approx 104$ mT (presumably due to VO^{2+} clusters) superimposed on HF lines due to isolated VO^{2+} ions. It is observed that the intensities of HF lines progressively increase in going from RT to LNT. It is also noted that HF lines are totally absent in the spectra for the 900 °C calcined sample. This indicates that the isolated VO^{2+} ions that have been left out drifted to connect to the already existing VO^{2+} clusters. RT spectra show isotropic HF structure which is explained as follows: isolated VO^{2+} ions attached to the surface of silica pores are involved in some kind of rotational motion and at a faster rate compared to the EPR timescale at RT, resulting in averaging out of the anisotropy in the HF splitting. The HF lines appearing at LNT show anisotropy in hyperfine constants (characterized by $A_\parallel$ and $A_\perp$) and signify that the rotational motion of VO^{2+} ions is damped down at LNT due to the freezing effect at low temperature.

From our optical findings described in the previous section 3(b)(II) (figure 6) the two bands (11 561 cm^{-1} and 15 385 cm^{-1}) for 700 °C calcined glass are typical for VO^{2+} ions and can be assigned to the $\Delta_\perp = {}^2B_{2g} \rightarrow {}^2E_g$ and $\Delta_\parallel = {}^2B_{2g} \rightarrow {}^2B_{1g}$ transitions, respectively. Both EPR and optical data can be used to calculate the molecular orbital (MO) bonding coefficients from the following equations [36–38]:

$$g_\parallel = g_e\left(1 - \frac{4\lambda\beta_1^2\beta_2^2}{\Delta_\parallel}\right) \quad (1)$$

$$g_\perp = g_e\left(1 - \frac{\lambda\gamma^2\beta_2^2}{\Delta_\perp}\right). \quad (2)$$

From the equations, it is seen that $g_\parallel$ and $g_\perp$ are related to the MO bonding parameters. β_1^2 and β_2^2 of the d^1 electrons, g_e (=2.0023) is the free electron g value and λ (=170 cm^{-1} [23, 39]) is the spin–orbit coupling constant of the VO^{2+} ion. The MO bonding coefficients β_1^2, β_2^2 and γ^2 characterize in-plane σ bonding, in-plane π bonding and out-of-plane π bonding, respectively [40].

The degree of distortion is estimated from the Fermi contact interaction parameter κ representing the amount of unpaired electron density at the vanadium nucleus. However, the unpaired electron present in d orbital causes a zero Fermi contact interaction. Because of the spin polarization of inner s-electrons, there exists a non-zero value of κ. The dipolar coupling parameter P is related to the radial distribution of the wavefunction of the ions: $P = g_e g_N \beta_e \beta_N \langle r^{-3}\rangle$. The parallel and perpendicular components of the hyperfine interaction, $A_\parallel$ and $A_\perp$, are related to the MO bonding coefficient β_2^2 [41]. MO coefficients for isolated vanadyl ions doped in a SiO_2 glass sample calcined at 700 °C are evaluated (table 2). The β_2^2, found in this work, indicates poor π bonding of the ligands. κ is lower than β_2^2, indicating that the delocalization of electrons is not great, so the in-plane π bonding ability of the ligand is poor. The κ value in the present case is less than in most of the other cases, which indicates mixing of the 4s orbital into the d_{xy} orbital. This may be due to the low-symmetry ligand field of C_{4v} symmetry. The term $(1-\beta_1^2)$ indicates the strength of σ bonding between vanadium atoms and equatorial ligands, while $(1-\gamma^2)$ indicates the strength of π bonding between the vanadium ion and the vanadyl oxygen. In the present case, the remarkably low value of $1-\beta_1^2$ is indicative of the strongly ionic in-plane σ bonding, whereas $1-\gamma^2$ suggests moderately ionic out-of-plane π bonding.

3.3.2. Type-II line. VO^{2+} ions form isolated clusters when pores begin to collapse at calcination temperatures $\geqslant$700 °C. In the VO_2 clusters VO^{2+} ions are exchange coupled. In consequence, HF structure is averaged out, resulting in the formation of a broad resonance spectrum. Computer simulation reveals that the RT broad symmetric resonance line (type-II) has an isotropic g-value ($\sim$2.0) and a larger linewidth ($\Delta H_{pp} \sim 104$ mT). Compared to the RT spectrum, the LNT spectrum shows quite a significant increase in linewidth ($\Delta H_{pp} \sim 250$ mT) without any perceptible line shift. The lineshapes of the spectra of these samples recorded at RT and LNT are approximately Lorentzian. In view of the powder XRD findings, the broad line has been assigned to nanosized VO_2 particles. The intensity of the EPR line shows an enormous increase in going from RT to LNT. Such an increase in EPR line intensity in going from RT to LNT suggests that the exchange coupling in these magnetic nanocrystals is of the ferromagnetic type.

It is worthwhile to correlate our VO^{2+} EPR findings with those obtained by Krol and Lierop [19] on size, specific surface area and volume/g of SiO_2 pores in undoped sol–gel silica glass as a function of heat treatment between 120 and 900 °C. In the undoped glass, a very significant rise in mean pore radius from 1.0 to 2.3 nm in going from the silica glass sample calcined at 700 °C to that calcined at 800 °C was found. A significant decrease in intensity of VO^{2+} HF lines also occurs in the sample calcined at 800 °C. The transformation to a nearly structureless broad line occurs at 900 °C. This may be explained as follows. At higher temperatures, i.e. $\geqslant$800 °C, quite a large number of small pores collapse resulting in the formation of VO_2 clusters and a single line EPR spectrum results. Also at the same time the remaining small pores assemble together to form larger pores. At still higher temperature, i.e. $\geqslant$900 °C, the collapse of larger pores takes place, similar to what has been observed in undoped SiO_2 glass as characterized by a rapid decrease of pore volume/g from 0.12 to 0.026 cm^3 g^{-1} in a temperature range from 800 to 900 °C. Raman spectral study has also indicated that the surface Si–OH groups have

Table 3. Magnetization data for V2 samples calcined at various temperatures.

Calcination temperature (°C)	Crystal size (nm) from TEM (see table 1)	Blocking temperature, T_B (K)	Irreversible temperature, T_{irr} (K)	Hysteresis (at 10 K)		Anisotropy constant, K (J m^{-3})
				H_c (T)	M_r (A m^2 kg^{-1})	
700	≈3	94	176	0.020	0.010	230×10^4
800	—	96	187	0.050	0.304	—
900	≈7	99	195	0.051	1.030	19×10^4

completely disappeared at such high temperatures, condensing to ≡Si–O–Si≡ bonds which engineer pore collapse. From the XRD data it is observed that irreversible transformation of some VO^{2+} ions to diamagnetic V_2O_5 is initiated at about 800 °C by oxidation and V_2O_5 nanocrystals are formed, and at 900 °C oxidation transformation of isolated VO^{2+} ions to diamagnetic V_2O_5 nanocrystals (d^0 configuration) is complete; as a result hyperfine structure due to VO^{2+} ions vanishes. The single broad line that remains in the 900 °C calcined sample is due to VO_2 nanocrystals.

3.4. Magnetization

The data obtained for the temperature dependence of the dc mass magnetization (ZFC and FC) of V2 samples calcined at 700, 800 and 900 °C in the presence of an applied dc magnetic field of 200 Oe in the 10–300 K temperature range are graphically represented in figure 8. Maxima in the ZFC mass magnetization curves for the samples calcined at 700, 800 and 900 °C are obtained at 94, 96 and 99 K, respectively. These characteristic temperatures are often referred to as the blocking temperatures (T_B), typical of this measurement technique. The occurrence of T_B has revealed the presence of the superparamagnetic phase of VO_2 NPs in these samples. Since NP size distribution is present, a spread in the blocking temperature may be rightly assumed, leading to the observed broad peak in the ZFC curve. T_B is found to occur below the irreversibility temperature T_{irr}, i.e. the temperature at which ZFC and FC curves bifurcate. Strictly, however, the irreversibility temperature T_{irr} is defined as the point where the ratio $[M_{FC}(T_{irr}) - M_{ZFC}(T_{irr})]/M_{FC}(T_{irr})$ is less than 1% [42]. From the observed continuous increase in FC magnetization with the lowering of the temperature below T_{irr}, it appears that VO_2 NPs have FM-like ordering below the irreversibility temperature. The shape of the curve differs from the usually found Curie-type behavior in other vanadate–lithium–borate glasses [6]. The higher T_B values indicate that the NPs have larger average energy barriers. Since the energy barrier is proportional to the volume, the larger T_B values signify that larger sized NPs are generated in the V2 samples treated at higher calcination temperatures. This is consistent with the XRD and TEM results. For the sample calcined at 700 °C, the ZFC curves starts to rise from 20 K with the further lowering of the temperature (figure 8(a)). Such an increase in magnetic moment may have originated from the paramagnetic contribution from a small number of isolated VO^{2+} ions present in the samples. The magnetic anisotropy constant K is estimated using the simple relation [43] $K = 25k_BT_B/V$, where k_B is the Boltzmann constant and V is the volume of the NP. V is calculated by taking the shapes of NPs as spheres, as is evident from TEM images. The estimated values are shown in table 3. It is significant to note that the magnetic anisotropy constant of the V2 sample calcined at 700 °C is greater (about 12 times so) than that of the sample calcined at 900 °C.

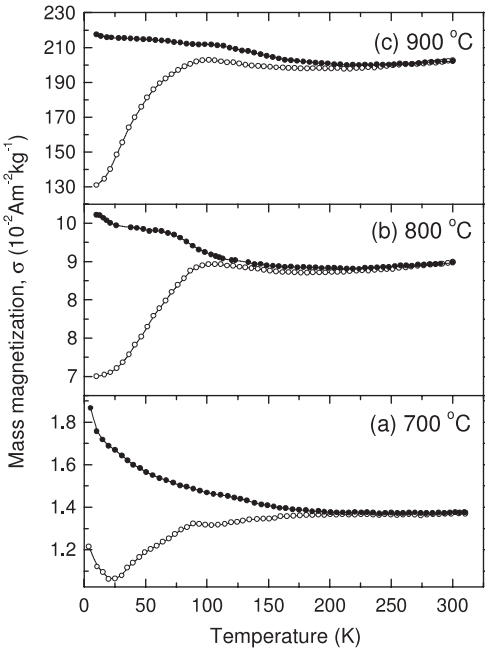

Figure 8. ZFC (○) and FC (●) mass magnetization versus temperature curves for V2 samples calcined at (a) 700 °C, (b) 800 °C and (c) 900 °C (applied DC magnetic field 200 Oe).

Studies on the field dependence of the magnetization of the samples calcined at 700, 800 and 900 °C in the magnetic field range ±5 T are carried out at two temperatures, namely 300 and 10 K (figures 9(a)–(c)). The values of coercive field (H_c) and remnant magnetization (M_r) evaluated from hysteresis loops are shown in table 3. For a sample calcined at 700 °C, the magnetization loop (zero area) obtained at 300 K displays characteristics of superparamagnetism. Below T_B, i.e. at 10 K, hysteretic behaviors are observed and the coercive field is found to have a non-zero value ($H_c = 0.020$ T). This means that at 10 K the NPs are in the magnetically ordered state. The above trend is more prominently displayed in the samples calcined at higher temperatures (figures 9(b) and (c)). This is evident from the bulging of the hysteresis loop near the central region (low field region) and also the magnetic moment/unit mass is enhanced compared to that at 300 K.

The hysteresis curves do not show any magnetic saturation in the magnetic field range of ±5 T, from which it is inferred

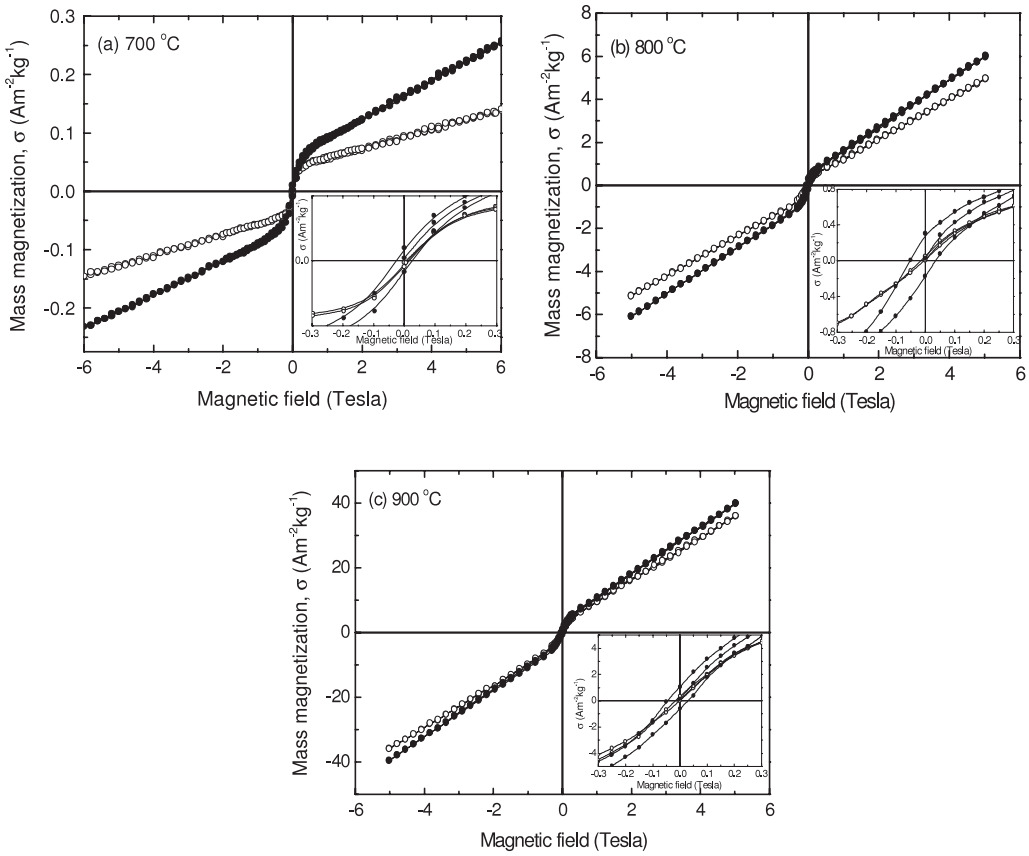

Figure 9. Hysteresis loops of V2 samples calcined at (a) 700 °C, (b) 800 °C and (c) 900 °C recorded at 300 K (○) and 10 K (●). In the inset, the region close to the displacement of the loop shift is highlighted.

that the VO_2 NPs contained in the samples possess large anisotropic fields [44, 45].

4. Conclusions

(i) It has been possible to successfully synthesize nanocrystalline VO_2 particles in silica glass matrices by a sol–gel method at calcination temperatures of 700 °C and above. The crystallinity of the particles and their sizes have been determined by XRD and TEM. VO_2 nanocrystals are obtained in larger sizes at higher calcination temperatures. From XRD studies, the presence of V_2O_5 nanocrystals in glass samples calcined at 800 °C has been confirmed, and is more prominent at higher calcination temperatures. Some IR bands which are characteristic of VO_2 particles have been identified.

(ii) From EPR and optical studies, it has been shown that V^+ ions in this SiO_2 glass system exist as isolated VO^{2+} ions in a square pyramidal confirmation with a tetragonal compression having C_{4v} symmetry. The optical spectra show three bands corresponding to the d–d transition $^2B_{2g} \rightarrow {}^2E_g(d_{xy} \rightarrow d_{xz,yz})$, $^2B_{2g} \rightarrow {}^2B_{1g}(d_{xy} \rightarrow d_{x^2-y^2})$ and $^2B_{2g} \rightarrow {}^2A_{1g}(d_{xy} \rightarrow d_{z^2})$. It is further seen that VO^{2+} ions are gradually oxidized to V^{5+} ions with increase in the calcination temperature. By correlating EPR and optical data, the MO coefficients for VO^{2+} have been evaluated. From the values of β_1^2 and γ^2, it is established that the in-plane σ bonding and out-of-plane π bonding are predominantly ionic in nature.

(iii) EPR spectra of V2 samples calcined at several temperatures in the temperature range 700–900 °C have depicted broad symmetric lines (ΔHpp:∼104 mT at RT and ∼250 mT at LNT), which have been assigned to VO_2 nanocrystals. The increment in VO_2 EPR intensity in going from RT to LNT suggests that VO_2 nanocrystals have ferromagnetic-like order at 77 K.

(iv) Investigations of the thermal dependence of magnetization (ZFC and FC) and magnetic hysteresis of VO_2:SiO2 glass calcined at 700, 800 and 900 °C have revealed that magnetic VO_2 nanocrystals present in these glasses display superparamagnetic–ferromagnetic transitions in the temperature interval 10–300 K. These studies have clearly shown the presence of superparamagnetic behavior for the sample calcined at 700 °C, the ferromagnetic transition being apparent at low temperature (∼10 K). Ferromagnetic effects are more prominently displayed in the samples calcined at higher temperatures.

References

[1] Ulrich D R 1990 *Chem. Eng. News* **68** 28
[2] Narasimhulu K V and Rao J L 1997 *Spectrochim. Acta* A **53** 2065
[3] Khasa S, Prakasa D, Seth V P, Gupta S K and Krishna R M 1997 *Phil. Mag.* B **76** 859

[4] Dhanuskodi S and Jeyakumari A P 2001 *Spectrochim. Acta* A **57** 971
[5] Ravikumar R V S S N, Rajagopal Reddy V, Chandrasekhar A V, Reddy B J, Reddy Y P and Rao P S 2002 *J. Alloys Compounds* **337** 272
[6] Cozar O, Ardelean I, Simon V, Ilonca G, Craciun C and Cefan C 2001 *J. Alloys Compounds* **326** 124
[7] Bogomolova L D and Jachkin V A 1983 *J. Non-Cryst. Solids* **58** 165
[8] Bogomolova L D, Jachkin V A, Lazukin V N, Pavlushkina T K and Shmuckler V A 1978 *J. Non-Cryst. Solids* **28** 375
[9] Bogomolova L D, Jachkin V A and Krasil'nikova N A 1998 *J. Non-Cryst. Solids* **241** 13
[10] Lopez R, Feldman L C and Haglund R F Jr 2004 *Phys. Rev. Lett.* **93** 177403
[11] Nogami M and Moriya Y 1980 *J. Non-Cryst. Solids* **37** 191
[12] Owen F J 1985 *Phase Transit.* **5** 81
[13] Seehra M S and Huber D L 1975 *Magnetism and Magnetism Materials* (*AIP Conf. Proc. No. 24*) ed C D Graham Jr, G H Lander and J J Rhyne (New York: AIP)
[14] Elschner B and Loidl A 1997 *Handbook on the Physics and Chemistry of Rare Earths* vol 24, ed K A Gschneider Jr and L Eyring (Amsterdam: North-Holland, Elsevier) chapter 162, p 221
[15] Taylor R H 1975 *Adv. Phys.* **24** 681
[16] Campbell I A, Hurdequint H and Hippert F 1986 *Phys. Rev.* B **33** 3540
[17] Toyuki H and Akagi S 1974 *Phys. Chem. Glasses* **15** 1
[18] Sakka S and Kamiya K 1982 *J. Non-Cryst. Solids* **48** 31
[19] Krol D M and van Lierop J G 1984 *J. Non-Cryst. Solids* **63** 131
[20] Bertoluzza A, Fagnano C and Morelli M A 1982 *J. Non-Cryst. Solids* **48** 117
[21] Simon I 1960 *Modern Aspect of the Vitreous State* vol 1, ed J D Mackenzie (London: Butterworths Scientific)
[22] Valmalette J C and Gavarri J R 1998 *Mater. Sci. Eng.* B **54** 168
[23] Ballhausen C J and Gray H B 1962 *Inorg. Chem.* **1** 11
[24] Ortolano D R, Selbin J and McGlynn S P 1964 *J. Chem. Phys.* **41** 262
[25] Narasimhulu K V and Rao J L 1997 *Spectrochim. Acta* A **53** 2605
[26] Satyanarayana N 1985 *Spectrochim. Acta* A **41** 1185
[27] Angeli Mary P A and Dhanuskodi S 2001 *Spectrochim. Acta* A **57** 2345
[28] Satyanarayana N and Radhakrishna S 1985 *J. Chem. Phys.* **83** 529
[29] Hecht H G and Johnston T S 1967 *J. Chem. Phys.* **46** 23
[30] Bleaney B, Bowers K D and Pryce M H 1995 *Proc. R. Soc.* A **228** 147
[31] Cozar O, Ardelean I and Ilonca G 1982 *Mater. Chem.* **7** 155
[32] Hosono H, Kawazoe H and Kanazawa T 1980 *J. Non-Cryst. Solids* **37** 427
[33] Abragam A and Bleaney B 1970 *Electron Paramagnetic Resonance of Transition Ions* (Oxford: Clarendon) p 175
[34] Muncaster R and Parke S 1977 *J. Non-Cryst. Solids* **24** 339
[35] Tiam F, Zhang X and Pan L 1988 *J. Non-Cryst. Solids* **105** 263
[36] Chakradhar R P S, Murali A and Rao J L 2000 *Physica* B **293** 108
[37] Seth V P, Gupta S, Jindal A and Gupta S K 1993 *J. Non-Cryst. Solids* **162** 263
[38] Muncaster R and Parke S 1977 *J. Non-Cryst. Solids* **24** 399
[39] Kivelson D and Lee S K 1964 *J. Chem. Phys.* **41** 1896
[40] Murali A, Rao J L and Subbaiah A V 1997 *J. Alloys Compounds* **257** 96
[41] Radhakrishna S and Salagram M 1980 *Phys. Status Solidi* a **62** 441
[42] Deac I G, Mitchell J F and Schiffer P 2001 *Phys. Rev.* B **63** 172408
[43] Cullity B D 1972 *Introduction of Magnetic Materials* (Reading, MA: Addison-Wesley) pp 410–8
[44] Li J, Wang Y J, Zou B S, Wu X C, Lin J G, Guo L and Li Q S 1997 *Appl. Phys. Lett.* **70** 3047
[45] Hadjipanayis G, Sellmyer D J and Brandt B 1981 *Phys. Rev.* B **23** 3349